Danmarks Tekniske Universitet

DTU

Assignment # 1
Turbulent flows

Authors

[redacted]

Szczepan Zygmunt Letkiewicz - s244067

November 18, 2024

Contents

1 Introduction **1**

2 Preliminary Flow Analysis **1**
2.1 Mean streamwise Velocity profile 1
2.2 Depth Averaged Velocity 2

3 Friction Velocity U_f **2**
3.1 Initial estimation 2
3.2 Verification 3

4 Dimensionless Velocity Distribution **4**
4.1 Van Driest comparison 5

5 Turbulence Quantities **5**
5.1 Flow behaviour for $0 \leq y^+ \leq 100$ 5
5.2 Flow behaviour for entire flow depth 6
5.3 Turbulent kinetic energy for entire flow depth 7

6 Reynolds Stress **8**

7 Simplified Energy Equation for Turbulence **9**

8 Comparison with experimental RANS model data **11**

9 Conclusion **12**

List of Figures **13**

References **13**

1 Introduction

This report presents an analysis of velocity measurements gathered using a two-component Laser Doppler Velocimeter (LDV), which captures the behaviour of a steady turbulent open channel flow. Specific details about the measurements and flow case can be found in Chapter 10 of Sumer and Fuhrman (2020) [1].

The analysis begins by evaluating the velocity profile and depth-averaged velocity, to establish a fundamental understanding of the flow. Next, the dimensionless friction velocity U_f is determined before being used to plot the dimensionless velocity distribution, which offers insight into the behaviour of the flow throughout the boundary layer. Following this, essential turbulence quantities are analysed across both the inner and outer regions, including an investigation of the turbulent kinetic energy. The Reynolds stress components and the turbulence energy equation are also explored in detail, before concluding the study with a comparison of the data with a RANS model.

2 Preliminary Flow Analysis

2.1 Mean streamwise Velocity profile

The mean velocity profile in the streamwise direction $\overline{u}(y)$ depicts the flow's behaviour with increasing wall-normal distance ($y-$direction).

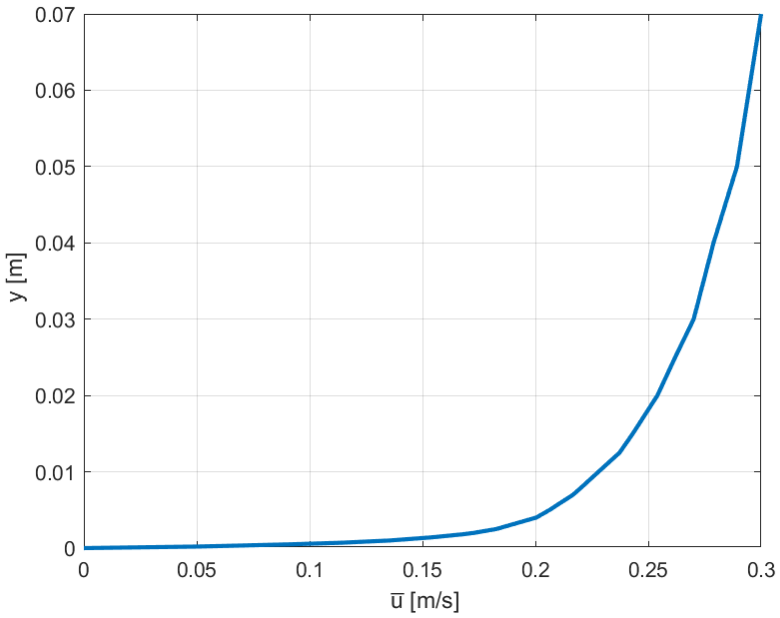

Figure 1: Streamwise velocity profile in the wall-normal direction.

Several flow features are identified by plotting $\overline{u}$ as a function of y (Figure 1). For instance, the graph shows a non-slip boundary condition at the wall, meaning that the flow

is stationary ($\overline{u}(0) = 0$) at this point. Additionally, the gradient of the velocity profile very near to the wall is initially shallow but increases rapidly beyond a certain point, when the shear stress is no longer the dominant factor. This is due to the fact that at very close distances to the wall, the energy is extracted from the flow by viscous forces and thus the velocity is low. Moving further away from the wall, these viscous effects are seen to lose strength quickly, leading to a rapid increase in $\overline{u}$. This velocity increase gradually tapers off after the constant stress region with increasing wall distance. This behavior is typical of turbulent flows. At small distances from the wall, it can be said that the gradient is approximately constant and equal to the wall shear stress $\tau_0 = \mu \frac{d\overline{u}}{dy}\big|_{y=0}$. This assumption is valid in the region close to the wall, which consists of three separate layers (Section 4) ranging from the wall to the point where shear stress is no longer constant, at approximately 10% of the channel height.

2.2 Depth Averaged Velocity

From the streamwise velocity profile presented in Subsection 2.1, the depth-averaged velocity V is calculated. Instead of measuring velocity at a single point, depth-averaged velocity considers the entire depth of the fluid column, providing a more comprehensive understanding of flow characteristics. By integrating the velocities over the entire flow depth, the depth-averaged velocity is found to be $V = 0.263$ m/s.

3 Friction Velocity U_f

3.1 Initial estimation

To plot the dimensionless velocity distribution in the upcoming section, the friction velocity U_f must first be estimated based on the previously determined depth-averaged velocity V. Friction velocity is a characteristic velocity parameter used to represent the shear stress exerted by the fluid on the wall. One method of estimating U_f for open channel flow is to look at the flow resistance, which depends on the Reynolds number Re of the flow (Equation 2). To calculate Re for this open channel flow, the hydraulic radius $r_h = A/P$ is needed [1]; where area $A = h \cdot b = 0.033$ m^2 and wetted perimeter $P = 2h + b = 0.440$ m. This results in a hydraulic radius of $r_h = 0.048$ m and consequently, a Reynolds number of $Re = 1.257 \times 10^4$.

The flow resistance relation is commonly expressed in terms of U_f (Equation 1), where the friction coefficient f is approximated from the Blausis formula (Equation 2).

$$U_f = \sqrt{\frac{f}{2}} V \qquad (1) \qquad\qquad f = \frac{0.0557}{Re^{0.25}} \qquad (2)$$

The estimated friction velocity is found to be $U_f = 0.0135$.

3.2 Verification

To verify the estimated friction velocity U_f, the mean velocity $\overline{u}$ from the LDV experiment data is plotted on a semi-log scale (Figure 2). The logarithmic layer of this velocity distribution is of particular interest for this analysis and can be easily described (Equation 3), featuring the constant $A = 2.5$.

$$\bar{u} = AU_f \cdot \ln y + B_1 \tag{3}$$

The logarithmic layer is bound by the region consisting of constant stress, and the point at which viscosity does not significantly affect the shear stress. Numerically the lower bound is taken to be at $y^+ = 30$, where viscous effects start to weaken and turbulent effects become significant. This value is an approximation taken from literature such that distance y is sufficiently large that the variation of the velocity $\frac{d\overline{u}}{dy}$ is independent of viscosity [1]. The upper bound is determined using the condition $y << h$, which is equivalent to the condition $y^+ << Re_\tau$, where $Re_\tau = \frac{hU_f}{\nu}$. It describes the previously mentioned constant shear stress region of approximately 10% of the height. For this flow case, $Re_\tau = 945.48$ hence why the bound is approximated to be $y^+ = 94.55 \approx 95$.

By fitting a straight line to the data in this region, the slope can be used to determine U_f. The linear approximation is found to be $\bar{u} = 2.5 \cdot 0.0132 \cdot \ln y + 0.381$, as shown in the plot (Figure 2).

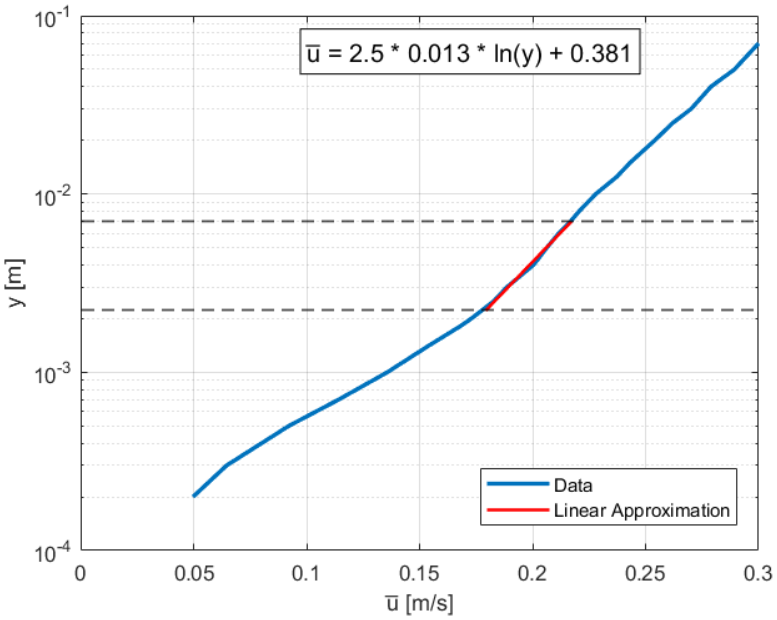

Figure 2: Velocity profile in logarithmic region.

The new U_f value is therefore calculated to be 0.0132, which is very similar to the previously estimated U_f of 0.0135 (Section 3.1), hence verifying the result.

4 Dimensionless Velocity Distribution

Implementing the friction velocity U_f, the velocity profile is replotted in a dimensionless fashion (Figure 3). Four distinct regions of the flow can be identified:

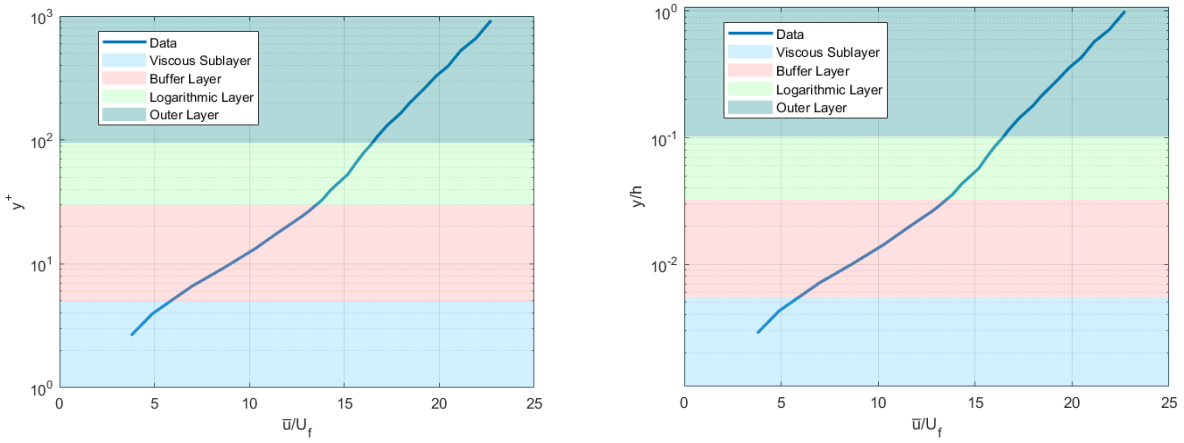

(a) y^+ (b) y/h

Figure 3: Dimensionless Velocity profile for $U_f = 0.0132$.

- Viscous sublayer $\rightarrow 0 < y^+ < 5$

The viscous sublayer is where the viscosity of the fluid is the dominant stress and prevents the turbulence from the flow's main body from penetrating the flow. Here the velocity varies linearly with the distance from the wall ($y^+ = \overline{u}/U_f$). The thickness of this layer is from the wall ($y^+ = 0$) to a thickness ($y^+ = 5$) where experiments show a deviation from the relation.

- Buffer layer $\rightarrow 5 < y^+ < 30$

In the buffer layer, the stress is caused by both turbulence and viscosity. This region's bounds are taken from the adjacent regions in agreement with experimental data. In this case, the upper bound is taken as $y^+ = 30$ such that distance y is sufficiently large that the variation of the velocity $\frac{d\overline{u}}{dy}$ is independent of viscosity. Literature [1] does, however, suggest that the upper bound can vary, potentially ranging between $5 < y^+ < 70$.

- Logarithmic layer $\rightarrow 30 < y^+ < 95$

See Section 3 for explanation.

- Outer region $\rightarrow 95 - \text{interval} < y^+ < h$

Lastly, the outer region satisfies the velocity distribution described by the velocity defect law ($\overline{u} = U_0 + U_f \cdot F_1\left(\frac{y}{h}\right)$). In this region, U_0 is the velocity at the free surface in the case of open channel flow. The outer layer and the logarithmic layer are expected to overlap in a certain y interval. This is because both regions rely on the same condition that viscosity drops with larger y.

4.1 Van Driest comparison

As a form of comparison, the LDA experimental data can be compared to the Van Driest model. This turbulence model is an empirical approximation because explicit expressions for the velocity distribution in the buffer layer are unavailable. The van Driest velocity distribution equation (eqn. 3.108 in [1]) is based on the mixing length model from Prandtl's mixing length hypothesis, an algebraic model that relates the size of turbulent eddies to velocity gradients by matching length scales and velocity scales.

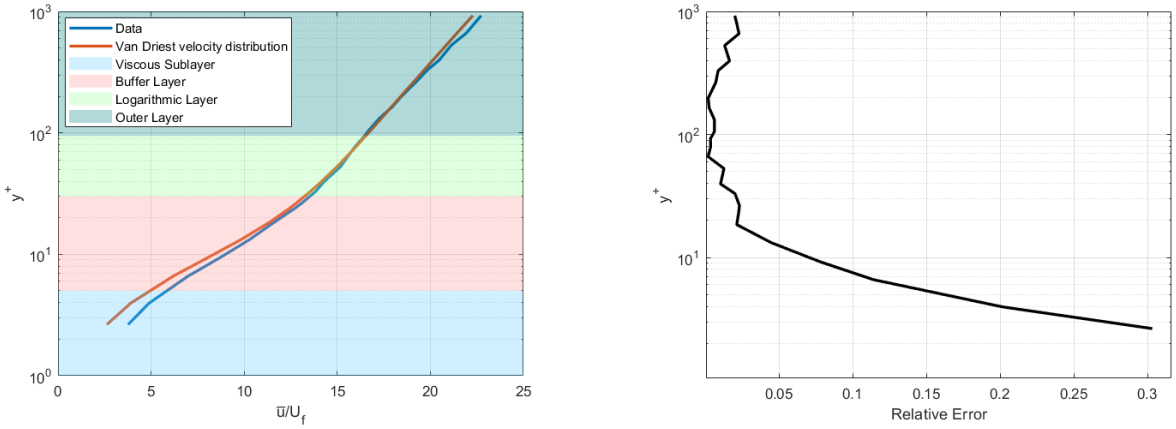

(a) Van Driest velocity distribution

(b) Error between data and van Driest

Figure 4: Dimensionless Velocity profile with Van Driest velocity distribution.

The van Driest profile shows agreement with the measured velocity profile (Figure 4a). In the buffer layer specifically, the relative error (Figure 4b) is seen to be especially small.

5 Turbulence Quantities

5.1 Flow behaviour for $0 \leq y^+ \leq 100$

Turbulence quantities $\overline{u'^2}, \overline{v'^2}, \overline{u'v'}$ are three independent Reynold stress components relevant for channel flow. To better understand the flow behaviour with respect to the dimensionless wall normal y^+, the root mean square of the values are taken and divided by U_f before plotting (Figure 5).

Based on wall-bounded flow theory, it is known that for large values of y^+, variation in velocity is independent of viscosity. Therefore, turbulence should also be independent, causing the quantities $\sqrt{\overline{u'^2}}/U_f, \sqrt{\overline{v'^2}}/U_f, \sqrt{-\overline{u'v'}}/U_f$ to tend to a constant with increasing y^+. The constants found are approximate, $A_1 \approx 1.9$, $A_2 \approx 1.1$ and $A_4 \approx 1$ respectively, and coincide with the findings of Sumer and Fuhrman [1].

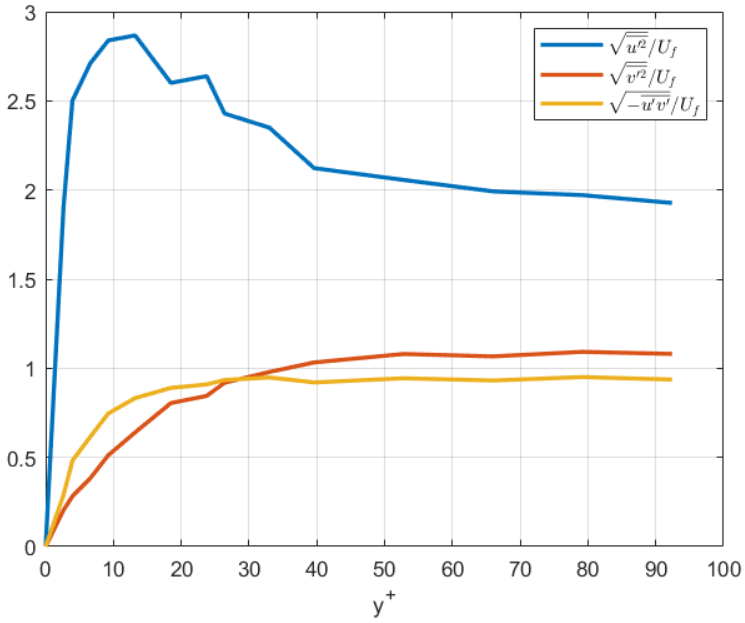

Figure 5: Root-Mean-Squared values of time-averaged turbulent fluctuations as a function of the normalized distance (y^+).

It is important to note that this asymptotic behaviour starts for the values of $y^+ = 40$-50, which indicates the presence of the logarithmic layer of the flow. Moreover, the highest fluctuation occurs for the turbulence quantity $\overline{u'^2}$ in the direction of mean flow velocity. Its maximum is reached in the viscous sublayer, indicated by small values of y^+.

5.2 Flow behaviour for entire flow depth

Similarly, these turbulence quantities can be visualized across the entire flow depth (Figure 6). The outer flow parameters are zero at the wall ($y = 0$) since no velocity fluctuations occur inside the wall. The quantities are also seen to decrease after the approximate 10 % of the flow depth, constant stress region, as the wall's presence becomes less significant on the flow behaviour.

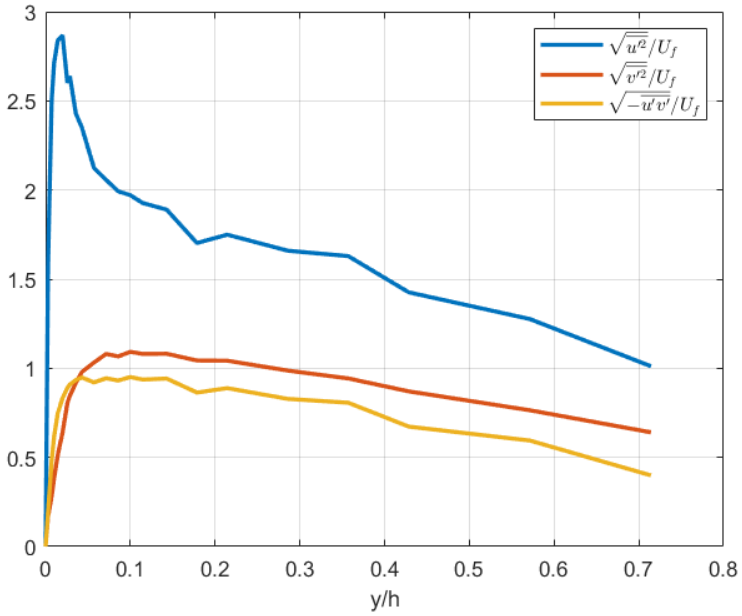

Figure 6: Root-Mean-Squared values of time-averaged turbulent fluctuations as a function of the water depth.

At the surface of the channel ($y = h$), the fluctuations are not provided in the data. However, at the surface the weaker velocity gradient of the flow (Figure 1) suggests that less turbulence generation occurs. Nevertheless, the flow is not entirely dissipated. Therefore it is expected that the quantity $\sqrt{\overline{u'^2}}/U_f$ is small but non-zero, $\sqrt{\overline{v'^2}}/U_f$ is even smaller but also non-zero, and $\sqrt{\overline{-u'v'}}/U_f$ is zero since the fluctuations u' and v' become uncorrelated.

From the figure, it can be concluded that the highest fluctuations occur for u'^2 close to the wall, since the flow in this direction is not restricted by the wall and therefore has the most turbulent energy.

5.3 Turbulent kinetic energy for entire flow depth

Determining the turbulent kinetic energy (TKE) per unit mass and plotting it against the channel depth (Figure 7) provides insight into how turbulent energy is distributed throughout the flow.

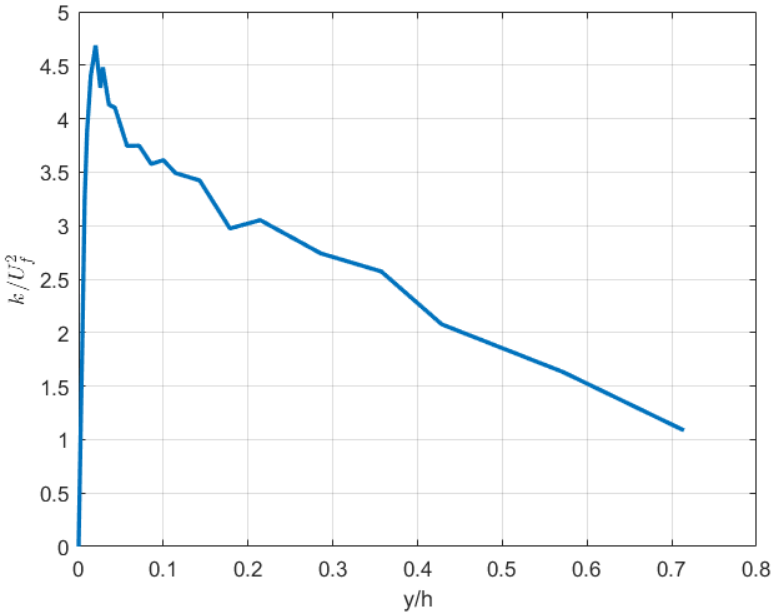

Figure 7: Normalized turbulent kinetic energy as a function of the water depth.

It can be shown that TKE achieves the highest values close to the wall, which stems from the fact that the highest turbulence fluctuations occur in that region. Moreover, it can be noticed that the shape of TKE is similar to the shape of turbulence fluctuation in mean flow direction $\overline{u'^2}$ (Figure 6), of which it is comprised.

Very close to the wall, a low TKE value is seen since the stress is dominated by viscous forces instead of turbulent fluctuations. As the distance from the wall increases the TKE is seen to increase in the buffer layer and reach its largest value as in the logarithmic layer. At the peak, the highest intensity of turbulent fluctuations is present due to developed turbulent structures. In the outer region, the TKE is seen to decrease as the turbulence is influenced by large-scale motions and less by wall effects.

6 Reynolds Stress

Reynolds stress $-\rho\overline{u'v'}$ is an off-diagonal term in Reynolds stress tensor corresponding to shear stress caused by a non-zero correlation between fluctuations in x-direction (u') and in y-direction (v'). Experimental and theoretical Reynolds stress curves as a function of the water depth are illustrated (Figure 8) to visualize the differences.

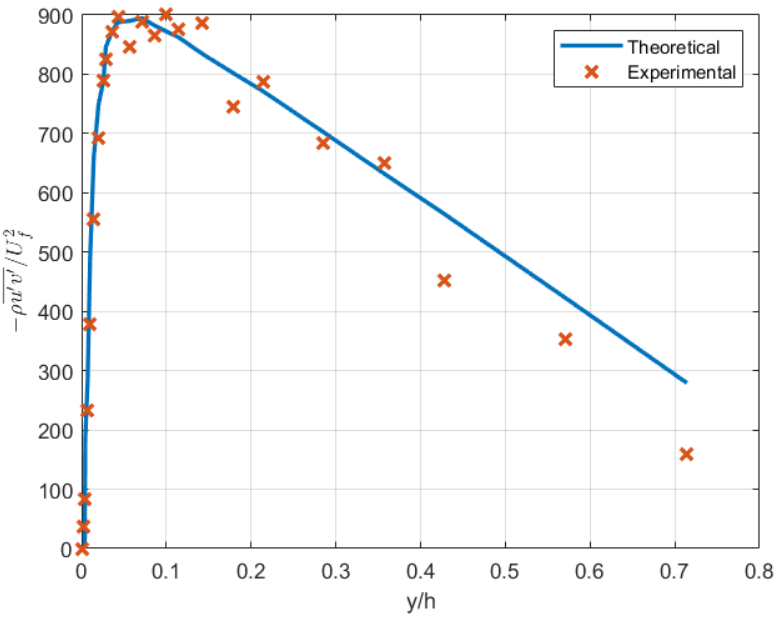

Figure 8: Reynolds stress as a function of the water depth.

Both curves follow a similar shape, where the highest Reynolds stress occurs for small values of the water depth. However, for large values of the water depth, experimental data shows lower stress values compared to the theoretical model. This may be because the theoretical model takes the mean shear stress, where in reality the shear stress is much lower close to the channel surface due to damping.

7 Simplified Energy Equation for Turbulence

The energy equation for turbulence describes the transport and dissipation of turbulent kinetic energy within a fluid flow. This equation, derived from the Reynolds-averaged Navier-Stokes (RANS) equations, expresses the rate of change of turbulent kinetic energy as a function of time and spatial variations, including terms for advection, production, dissipation, and pressure-strain effects. It can be displayed in Einstein notation as follows [1]:

$$\begin{aligned}\frac{\partial K_t}{\partial t} + \frac{\partial}{\partial x_\alpha}\left[K_t\overline{u_\alpha} + \frac{1}{2}\rho\overline{u_i'u_i'u_\alpha'} + \overline{p'u_\alpha'} - \overline{u_i'\mu\left(\frac{\partial u_i'}{\partial x_\alpha} + \frac{\partial u_\alpha'}{\partial x_i}\right)}\right] \\ = \rho\overline{u_\alpha'g_\alpha'} - \Phi_t + \left(-\rho\overline{u_i'u_\alpha'}\right)\frac{\partial \overline{u_i}}{\partial x_\alpha}\end{aligned} \tag{4}$$

where K_t represents the kinetic energy of turbulence:

$$K_t = \frac{1}{2}\rho\overline{u_i'u_i'} \tag{5}$$

and Φ_t represents the viscous dissipation of the turbulent energy:

$$\Phi_t = \mu \overline{\left(\frac{\partial u' i}{\partial x \alpha} + \frac{\partial u'_\alpha}{\partial x_i} \right) \frac{\partial u'_i}{\partial x_\alpha}} \tag{6}$$

For the flow under consideration, a number of assumptions and simplifications can be made. Firstly, the flow is considered to be steady, meaning that the flow properties will remain constant over time ($\frac{\partial}{\partial t} = 0$). Furthermore, the flow is taken to be streamwise uniform for the entire length of the flume, meaning that the flow properties will remain constant in the streamwise (x) direction ($\frac{\partial}{\partial x} = 0$).

In addition, it can also be assumed that the mean vertical velocity will remain constant over the height, as the flow is predominantly driven by horizontal forces, and vertical variations are negligible in this case.

Lastly, even though turbulence is a 3D phenomenon, the flow is considered a 2D case, meaning that any flow velocities in the z-direction, can be neglected ($z = 0, \frac{\partial}{\partial z} = 0$). These assumptions cause the following changes in the energy equation.

$$\frac{\partial u_i}{\partial t} = 0, \frac{\partial u_i}{\partial x} = 0, \frac{\partial \overline{v}}{\partial y} = 0, \frac{\partial u_i}{\partial z} = 0,$$

This results in the x and z directions cancelling out, providing no meaningful results. However, when applied to the y-direction, the turbulence energy equation produces the following:

$$\begin{aligned} \frac{\partial}{\partial y} \left[\frac{1}{2} \rho \overline{v} \left(\overline{u'u'} + \overline{v'v'} \right) + \frac{1}{2} \rho \left(\overline{u'u'v'} + \overline{v'v'v'} \right) + \overline{p'v'} - \overline{\mu \left(u' \frac{\partial u'}{\partial y} + 2v' \frac{\partial v'}{\partial y} \right)} \right] \\ = \rho \overline{v} \overline{g_y} - \overline{\mu \left[\left(\frac{\partial u'}{\partial y} \right)^2 + 2 \left(\frac{\partial v'}{\partial y} \right)^2 \right]} - \rho \overline{u'v'} \frac{\partial \overline{u}}{\partial y} \end{aligned} \tag{7}$$

From Equation 7, the term:

$$-\rho \overline{u'v'} \frac{\partial \overline{u}}{\partial y}$$

is of special interest. This term represents an energy gain for turbulence, or conversely an energy loss for the mean flow. This can be expressed as a function of the height (Figure 9).

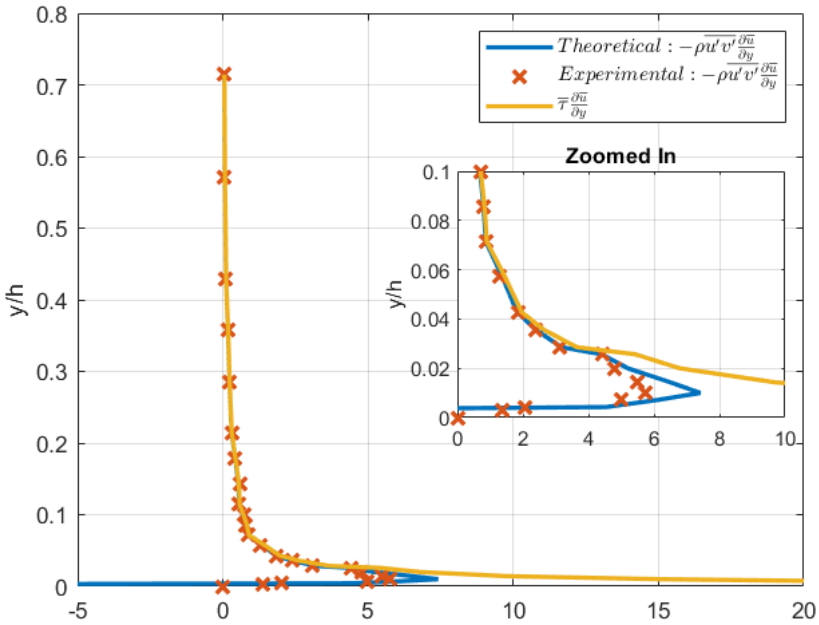

Figure 9: Energy gain for turbulence as function of water depth.

Figure 9 shows the experimental data along with the theoretical energy equation. Furthermore, using the mean shear stress formula provided in [1], the expected shear stress is also plotted for reference.

For the flow in question, the boundary layer near the channel's bottom wall experiences the most intense interaction between the fluid and the surface, resulting in higher shear stresses. Higher shear stresses result in more production of turbulence because they indicate a greater velocity gradient between adjacent layers of fluid, leading to instability and the breakdown of smooth flow into chaotic eddies and vortices. This relation coincides with the expected behaviour shown in Figure 2.2c from [1].

8 Comparison with experimental RANS model data

A comparison between a turbulence model and experimental data is often made to validate turbulence models and analyze the behaviour of the flow. Here, the Reynolds-averaged Navier-Stokes k-ω model is being evaluated.

Two characteristic properties of the flow are plotted against the water depth y/h (Figure 10). These include the mean flow velocity in the x-direction $\overline{u}$ (Figure 10a) and the turbulent kinetic energy k, normalized by the frictional velocity U_f (10b) .

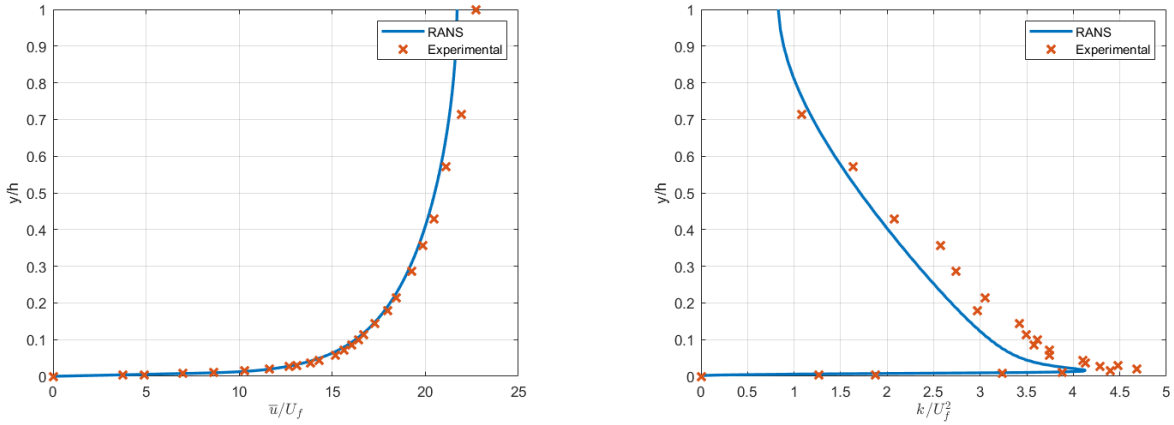

(a) Mean flow velocity in the x-direction

(b) Tubulent kinetic energy

Figure 10: Characteristic properties of the flow as a function of the water depth.

In both cases, the shape of experimental data curves coincides well with modelled data. A stronger correlation is present for the mean flow velocity, whereas the turublent kinetic energy differs significantly close to the wall. This is likely caused by the assumptions made in the modelling of the velocity fluctuations and Reynolds stresses.

9 Conclusion

In conclusion, this report provides a comprehensive analysis of steady turbulent open channel flow based on velocity measurements using a two-component Laser Doppler Velocimeter (LDV). The study examines the velocity profile, depth-averaged velocity, and friction velocity, with further exploration of dimensionless velocity distributions. Key turbulence quantities, including Reynolds stress components and turbulent kinetic energy (TKE), are analyzed, providing valuable insights into flow behaviour across different flow regions. The comparison with the Van Driest model and the subsequent validation of results highlights the consistency between experimental data and theoretical models, offering a robust understanding of turbulent flow dynamics.

List of Figures

1 Streamwise velocity profile in the wall-normal direction. 1
2 Velocity profile in logarithmic region. 3
3 Dimensionless Velocity profile for $U_f = 0.0132$. 4
4 Dimensionless Velocity profile with Van Driest velocity distribution. 5
5 Root-Mean-Squared values of time-averaged turbulent fluctuations as a function of the normalized distance (y^+). 6
6 Root-Mean-Squared values of time-averaged turbulent fluctuations as a function of the water depth. 7
7 Normalized turbulent kinetic energy as a function of the water depth. 8
8 Reynolds stress as a function of the water depth. 9
9 Energy gain for turbulence as function of water depth. 11
10 Characteristic properties of the flow as a function of the water depth. 12

References

[1] B. M. Sumer and D. R. Fuhrman, *Turbulence in Coastal and Civil Engineering*. Advanced Series on Ocean Engineering, World Scientific, 2020.